A study of double facades with phase-change storage and photovoltaics

A.K. Athienitis, J. Zhang and D. Feldman
Department of Building, Civil & Environmental Engineering, Concordia University, Montreal, Quebec, Canada

ABSTRACT

This paper considers a double facade for preheating of fresh air, generation of electricity with integrated photovoltaic panels and storage of solar energy in phase-change material - butyl stearate absorbed in gypsum board. A simple transient numerical control volume model is developed for the heat transfer in the PCM. Different facade systems are studied with computer simulations and full scale experiments. Combinations with photovoltaics are then considered. Solar utilization efficiencies of up to 70% are obtained.

1. INTRODUCTION AND BACKGROUND

Solar energy collection and utilization systems that constitute an integral part of the building envelope or interior walls and floors save in installation and material costs. Façade-integrated photovoltaic panels may be utilized to generate electricity and useful heat (Loret et al., 1995), with possible efficiencies of nearly 70% in some cases (Charron and Athienitis, 2003). In addition, building-integrated thermal storage, particularly phase-change materials, can be an effective means of reducing peak loads and controlling associated temperature fluctuations (Athienitis and Santamouris, 2002).

Recent developments that facilitate building integration include microencapsulated PCM that can be mixed with plaster and applied to interior surfaces (Schossig et al., 2004) and solid-solid transition materials (Van Oort and White, 1988).

An outdoor test facility has been developed with two configurations of the double facade with photovoltaic panels - with the PV panel forming the outside layer of the opaque wall section and airflow behind it (configuration 1) and with the PV panel in the middle of a glazed cavity and outside air flowing on both sides of the panel (configuration 2) as shown in Figure 1.

The façade combinations of interest in the present paper include combinations of photovoltaic panels with air flow behind the PV (configuration 1) or on both sides of the PV (configuration 2). This paper focuses primarily on configuration 2 with and without PCM.

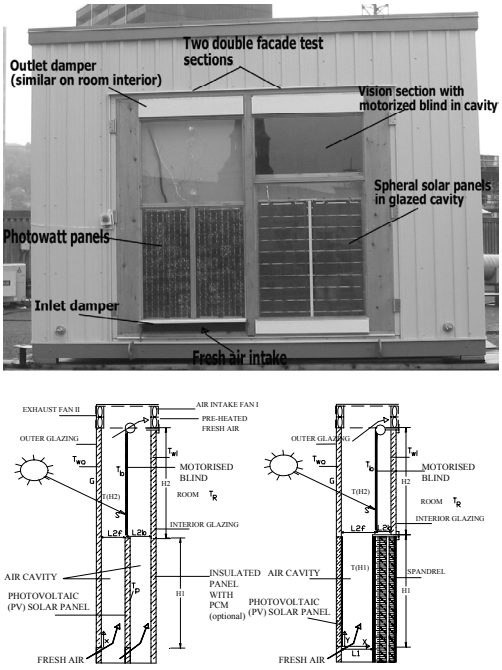

Figure 1: Top: Solar façade test facility; Bottom: Two configurations for tests indicating some components – PV panels, blinds and PCM gypsum board location.

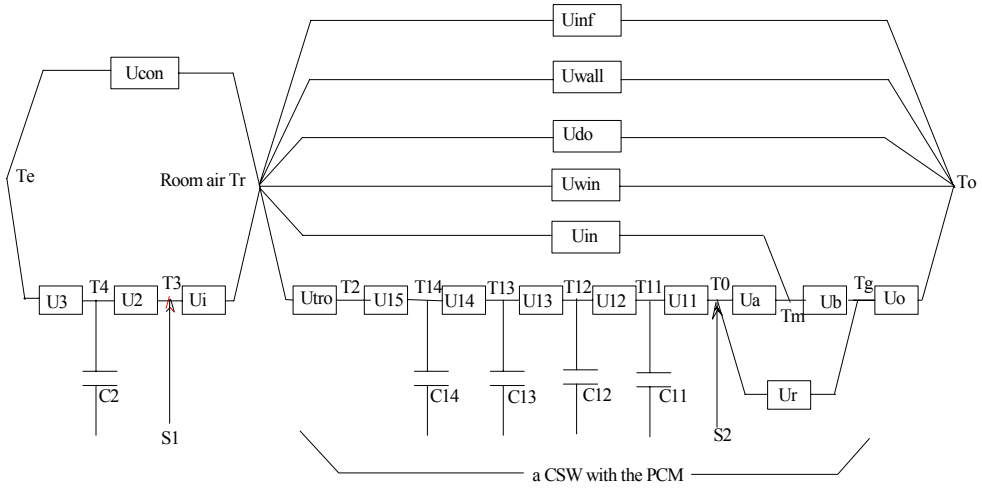

Figure 2: Thermal network of room with collector-storage wall with phase-change thermal storage and ventilated cavity.

Heat transferred to the air in the cavity occurs through convection and advection; the enthalpy gained in the cavity elements is obtained as:

$$Q_{air} = m_a \cdot \rho_a \cdot c_a \cdot (T_{out} - T_{in}) \qquad (1)$$

where m_a is an airflow rate of air, ρ_a represents the air density, and c_a is the specific heat capacity of air (J/kg.K). The solar energy utilization efficiency of the collector-storage wall (CSW) system with a PCM and photovoltaic panels can generally be expressed with the following equation:

$$\eta = \frac{E_{pv} + Q_{air} + Q_{sto} - E_{fan}}{S \cdot A} \qquad (2)$$

where E_{pv} is the electrical output of photovoltaic(PV) panels integrated with the CSW, Q_{air} is the heat absorbed by flowing air in the CSW, Q_{sto} is heat stored in the PCM in this cavity and E_{fan} is electrical fan power.

2. NUMERICAL SIMULATION MODEL

We present (see Fig. 2) a generalized thermal network model of a façade with a motorized blind, phase-change thermal storage connected with a room. The façade is used to preheat the air. The model corresponds to configuration 2 but without the upper section and with the PV panel removed and PCM on the back panel. The PCM is discretized into four control volumes (four thermal capacitances C11, C12, C13 and C14 plus interconnecting conductances. Tm represents the mean temperature of the air flowing in the cavity. Uinf, Uwin, and Uwall represent the conductance of the infiltration, the window and the wall (including the roof). Qaux is the auxiliary heat source. Using explicit (forward) differencing, the energy balance for each node (control volume) i is as follows:

$$C_i \cdot \frac{T_{p+1} - T_p}{Dt} = \sum U_{i,j} \cdot (T_{j,p} - T_{i,p}) + q \qquad (3)$$

where subscript j denotes the nodes that are connected to the node i, p is the time step, $U_{i,j}$ is the thermal conductance between nodes i and j, C_i is the thermal capacitance associated with node i, q represents heat source at node i (the source could be solar radiation, latent heat or auxiliary heat). During the freezing phase of the PCM, heat is released, so q is positive; during thawing phase, heat is absorbed and q is negative (see Athienitis et al., 1997 for a model for q). To ensure numerical stability, the time interval is selected based on the following condition:

$$\Delta t \le \min\left[\frac{C_i}{\sum_j (U_{i,j})}\right] \text{ for all nodes i} \qquad (4)$$

where Ui,j is the thermal conductance between

nodes i and j.

The gypsum board (13 mm thick) soaked with butyl stearate has approximately the properties described by Athienitis et al., (1997). The latent heat L and the transition temperatures Tin and Tfa are the most important parameters for phase change materials. They are the basis of the thermal analysis of phase change materials. In the present study, a DuPont 910 Differential Scanning Calorimeter (DSC) was used to measure these parameters. L was found to be 29.1 J/g, the melting interval was 16.8~20.9 ºC, while the freezing range was 19.2~17.0 ºC. The thermal conductivity of the PCM board was approximately 0.18 W/m.K. Although the samples were made in 1995 for use in the earlier study by Athienitis et al., (1997) there was very small (less than 2%) change in their properties.

3. RESULTS AND DISCUSSION

The model described above was validated by comparing with experiments as shown in Figure 3 and was subsequently utilized in simulation studies of several combinations of interest. The average air velocity was 0.65 m/s (forced

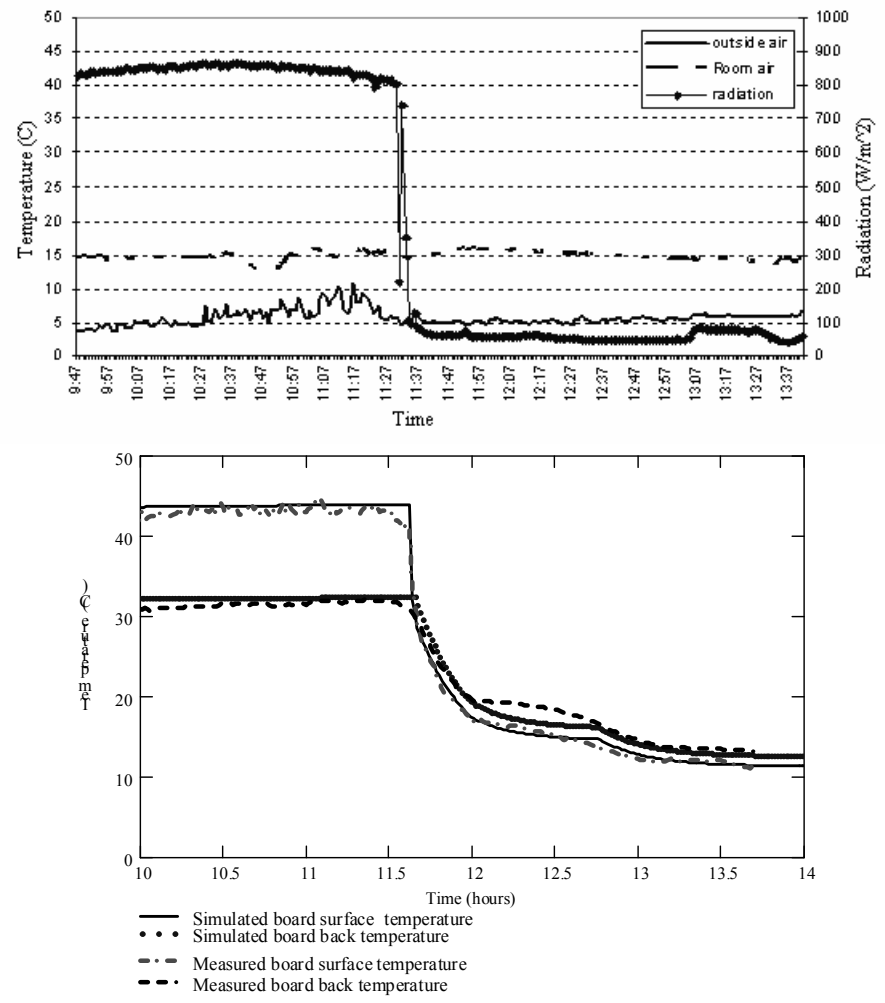

Figure 3: Top: Measured weather data on Nov. 10, 2003. Bottom: Comparison of predicted and simulated temperatures of PCM gypsum board during freezing on Nov. 10, 2003.

convection). The PCM board was installed to leave an air space of 0.09m from the outside glazing in configuration 2 (with PV removed). The height and width of the PCM board are approximately 1.12m x 0.9m. A single layer of glazing covers the cavity, forming a 0.09m air gap.

In this particular case, the solar utilization efficiency over the period of interest is 66%.

The combined thermal-electric efficiency of the facade is approximately 35-40% for configuration 1 and 65-70% for configuration 2 (with PV panels with an efficiency of 10%). In configuration 2, PCM was added for several experiments. The PCM was added to configuration 2 for several experiments to reduce the rise in temperature of the PV panels. This was achieved - the maximum temperature was reduced significantly, the reduction depending on flow rate. Experimental and simulation results were in reasonably good agreement as in Figure 3. Figure 4 shows representative results from the BIPV tests on a cold March day.

The above experimental results indicate that even on a cool day the temperature of the PV panel approached 56ºC in configuration 2. Given that the electrical conversion efficiency of silicon PV drops by about 1% (e.g. from 12% to 11%) for 25ºC rise in temperature, it is advantageous to cool the panels. This objective can be achieved by controlling the airflow and with PCM storage possibly attached to the panels – a case now being investigated.

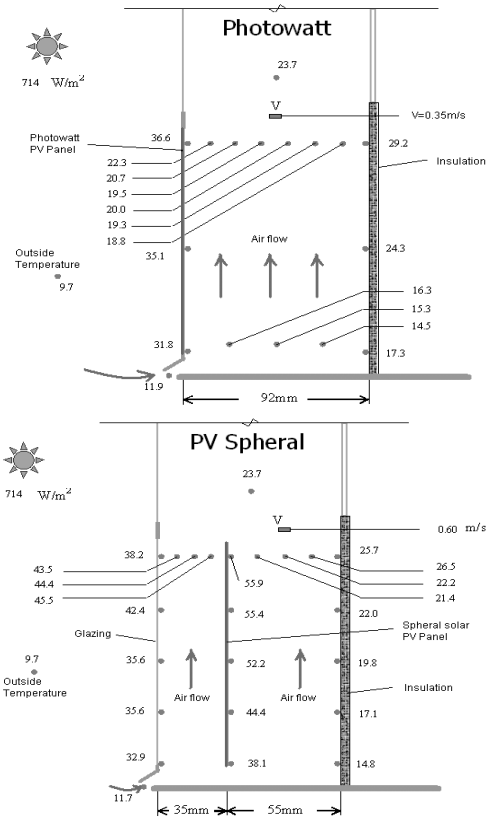

Figure 4: Experimental results for BIPV test Configurations 1 (top) and 2 (bottom) on March 29th, 2004 (numbers indicate temperature of surfaces and air in °C); solar radiation is total incident on vertical surface; V is average velocity.

4. CONCLUSIONS

This paper presented a study of an innovative façade system including photovoltaic solar panels, phase-change thermal storage and blinds. A numerical simulation model was presented and compared with simulation results for a façade with PCM, showing good agreement. Experimental results for BIPV facades showed potential solar utilization efficiencies approaching 70% (thermal plus electric).

ACKNOWLEDGEMENTS

Financial support for this collaborative research project was provided in part by Natural Resources Canada through the Innovative Research Initiative and the Technology and Innovation Program as part of the climate change plan for Canada. ATS (Spheral Solar Power Inc.), NSERC (Strategic grant) and CANMET (CETC Varennes) also provided extensive support for this project.

REFERENCES

Athienitis, A.K. and M. Santamouris, 2002. Thermal Analysis. and Design of Passive Solar Buildings, James and James, London, UK.

Athienitis, A.K., C. Liu, D. Hawes, D. Banu and D. Feldman, 1997. Investigation of the Thermal Performance of a Passive Solar Test-room with Wall Latent Heat Storage. Building and Environment, Vol. 32, No. 5, pp. 405-410.

Charron, R. and A.K. Athienitis, 2003. Optimization of the Performance of PV-Integrated Double Façades. ISES Solar World Congress, Goteborg, Sweden, June.

Loret et al., 1995. The Mataro public library: a 53 KW grid connected building with integrated PV–thermal multifunctional modules. 13th European PV Solar Energy Conference, Nice, France, 490-493.

Schossig, P., H. Henning and T. Haussmann, 2004. Microencapsulated Phase Change Materials integrated into construction materials. Proceedings of Eurosun, European Solar Energy Conf., Freiburg, Germany, June.

Van Oort, M.J.M. and M.A. White, 1988. Ber. Bunseges. Phys. Chem. 93, 168-176.